

Universal Dense-Matter Trace Anomaly Inferred from Collective Flow in Heavy-Ion Collisions and Global Properties of Neutron Stars

Bao-An Li^{1,*}

¹*Department of Physics and Astronomy, East Texas A&M University, Commerce, TX 75429-3011, USA*

(Dated: January 21, 2026)

The trace anomaly of dense matter, $\Delta \equiv 1/3 - P/\varepsilon$, defined in terms of the ratio of pressure P to energy density ε , quantifies deviations from conformal symmetry and plays a central role in both the hydrodynamic response and gravitational equilibrium. While $\Delta(\varepsilon)$ has recently been inferred from neutron star observations, we report the first Bayesian extraction of the trace anomaly from collective flow observables in intermediate-energy heavy-ion collisions. By employing transport-model simulations that explicitly decouple the cold-matter mean-field potential from thermal effects, we directly constrain the cold dense-matter equation of state (EOS). Remarkably, the trace anomaly inferred from laboratory flow data agrees quantitatively, within 68% credible intervals, with independent astrophysical posterior bands. This nontrivial agreement demonstrates that heavy-ion collisions and neutron star observations probe the same universal macroscopic properties of dense matter, establishing the trace anomaly as a composition-insensitive descriptor of dense matter across widely different physical environments.

Introduction.—Understanding the nature of supradense nuclear matter and its EOS, encoded in the pressure–energy density relation $P(\varepsilon)$, is a longstanding challenge shared by nuclear physics and astrophysics. In the gravitational regime, the $P(\varepsilon)$ relation determines the internal structure of neutron stars through the Tolman–Oppenheimer–Volkoff (TOV) equations [1, 2]. Recent progress has shifted attention toward constraining the dimensionless trace anomaly $\Delta \equiv 1/3 - P/\varepsilon$ [3], which characterizes deviations from conformal behavior and the approach to the asymptotic limit predicted by perturbative QCD at high densities [4–12].

A central difficulty in this endeavor is composition degeneracy: macroscopic observables such as neutron star masses, radii, and tidal deformabilities depend on the EOS $P(\varepsilon)$ but are largely insensitive to its microscopic origin, whether nucleonic, hyperonic, or quark matter [13]. This degeneracy, however, suggests that $\Delta(\varepsilon)$ may serve as a particularly robust and universal descriptor of dense matter. While recent astrophysical analyses have begun to constrain this quantity, an independent, non-gravitational probe is essential for establishing its universality.

In this Letter, we provide such an independent test by performing a Bayesian inference of the cold dense-matter trace anomaly from collective flow observables [14–16] in heavy-ion collisions. Collective flow encodes the integrated response of strongly interacting matter to pressure gradients over the full space–time evolution of the collision. We show that the trace anomaly extracted from laboratory data at GSI (FOPI [17] and HADES [18]) is quantitatively consistent with constraints inferred from GW170817 and NICER observations. This agreement identifies $\Delta(\varepsilon)$ as a unifying macroscopic property linking femtometer-scale nuclear dynamics to kilometer-scale neutron star structure. While trace-anomaly-related quantities have been extensively

studied in high-temperature quark–gluon plasma created at ultrarelativistic energies, this work presents the first Bayesian extraction of the cold dense-matter trace anomaly from collective flow in heavy-ion collisions and its quantitative agreement with independent neutron star constraints.

Intrinsic composition degeneracy of TOV equations and neutron star global observables.—The TOV equations (with $c = 1$) [1, 2]

$$\frac{d}{dr}P = -\frac{G(\varepsilon + P)(M + 4\pi r^3 P)}{r^2(1 - 2GM/r)}, \quad \frac{d}{dr}M = 4\pi r^2 \varepsilon \quad (1)$$

govern the internal structure and global observables of neutron stars. Especially since GW170817, great progress has been made not only in narrowing down the $P(\varepsilon)$ band, but also more recently, in constraining the dimensionless ratio $\phi \equiv \frac{P}{\varepsilon}$ which determines the trace anomaly $\Delta(\varepsilon)$ [3]. With sound speed squared $c_s^2(\varepsilon) \equiv \frac{dP}{d\varepsilon}$, the ratio ϕ represents the energy-density–averaged sound speed squared $\langle c_s^2(\varepsilon) \rangle$ [19, 20]:

$$\langle c_s^2(\varepsilon) \rangle = \frac{1}{\varepsilon} \int_0^\varepsilon c_s^2(\varepsilon') d\varepsilon' = \frac{P(\varepsilon)}{\varepsilon} = \phi(\varepsilon). \quad (2)$$

Perturbative QCD (pQCD) predicted that Δ approaches zero from above at asymptotically high densities, reflecting the approximate restoration of conformal symmetry of quark matter [4–12]. Moreover, General Relativity (GR) sets a lower limit of $\Delta_{GR} \geq -(0.041 \sim 0.051)$ [21–23]. These two limits are indicated in Fig. 1.

The TOV equations are intrinsically composition degenerate, namely, they only see the $P(\varepsilon)$ but not its microscopic origin. Whether the pressure comes from nucleons, hyperons, quarks, two-body forces, three-body forces, short-range correlations, or other sources is irrelevant unless they uniquely change the EOS itself. While in

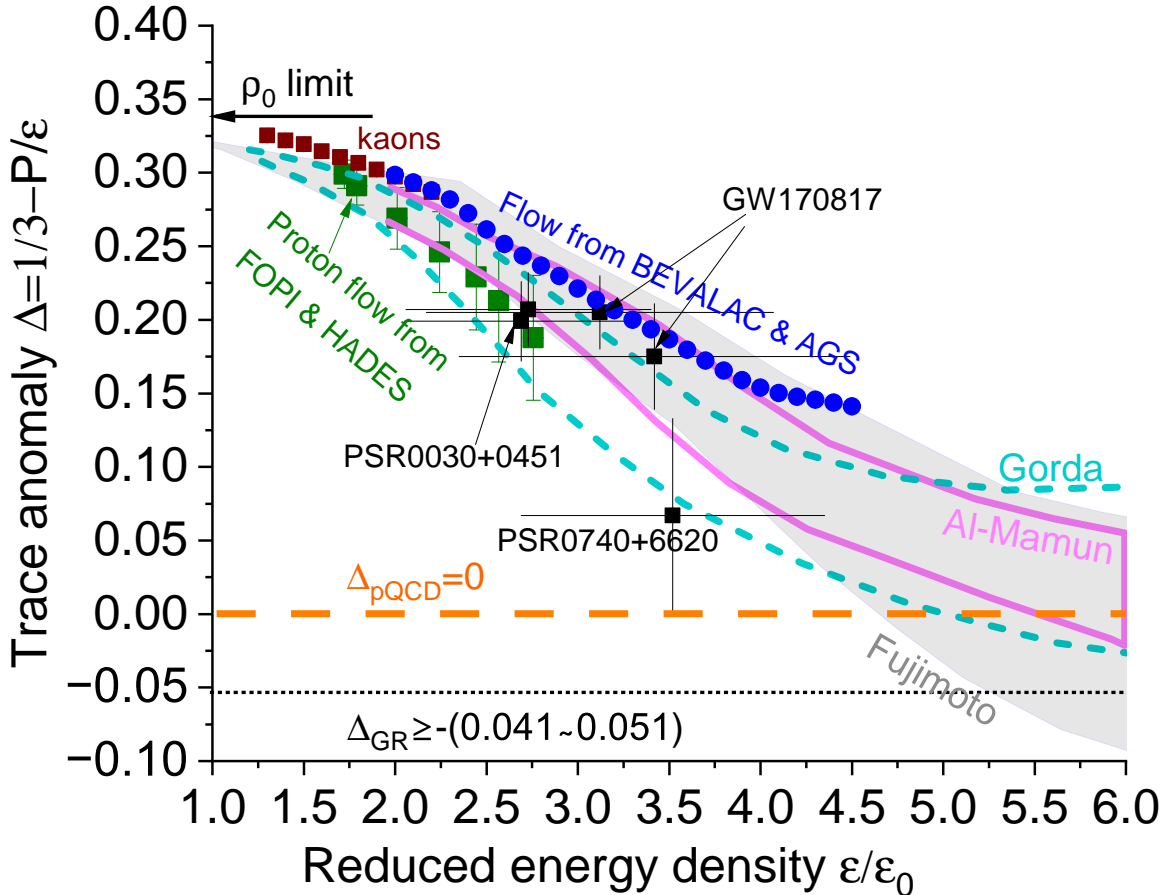


FIG. 1. Trace anomaly $\Delta(\varepsilon)$ as a function of reduced energy density. Values are shown as inferred from Bayesian analyses of neutron star observational data by (1) Gorda *et al.* [8], (2) Al-Mamun *et al.* [24], and (3) Fujimoto *et al.* [3]. Also plotted are the central $\Delta(\varepsilon)$ values [25] for the binary neutron stars GW170817 [26], PSR J0030+0451 [27, 28], and PSR J0740+6620 [29]. These astrophysical constraints are compared with Bayesian-inferred $\Delta(\varepsilon)$ values (green squares) obtained from proton collective flow data measured by the FOPI and HADES Collaborations at GSI [17, 18]. For historical context, we also include $\Delta(\varepsilon)$ values obtained by converting the continuous pressure bands previously extracted through forward-modeling of kaon production [30, 31] and collective flow at BEVALAC and AGS energies [32]. The pQCD and GR limits, as well as $\Delta(\rho_0) = 1/3$ are indicated by the horizontal lines.

forward modeling of neutron stars, one can use a chosen microscopic model to construct a unique EOS to predict observables (e.g., mass, radius, tidal deformation), the inverse inference from observables to microscopic models is not unique. Fundamentally, the forward modeling tells us how a given microscopic theory maps into observables. But inverse inference tells us what part of the theory survives coarse-graining. That surviving part from analyzing neutron star global observables is $P(\varepsilon)$ and its derivatives, but not the underlying Hamiltonian. Thus, neutron star observables constrain the macroscopic EOS, while each forward modeling provides one possible microscopic realization consistent with it. Unlike the EOS $P(\varepsilon)$ itself, the trace anomaly Δ is dimensionless, insensitive to absolute energy scales and additive constants in ε , and weakly sensitive to how kinetic vs potential energy is split. Moreover, because many microscopic differences modify P and ε in correlated ways, these variations largely cancel in the ratio ϕ , making $\Delta(\varepsilon)$ significantly more model-independent than the EOS itself.

Indeed, the $\Delta(\varepsilon)$ inferred recently from neutron star observations using various Bayesian frameworks constrained by chiral effective field theory at low densities and perturbative QCD at high densities, yielded mutually consistent results across several independent analyses as illustrated by three examples in Fig. 1 from Gorda *et al.* [8], Al-Mamun *et al.* [24] and Fujimoto *et al.* [3]. Shown also are the central $\Delta(\varepsilon)$ values [25] in the

Indeed, the $\Delta(\varepsilon)$ inferred recently from neutron star observations using various Bayesian frameworks constrained by chiral effective field theory at low densities and perturbative QCD at high densities, yielded mutually consistent results across several independent analyses as illustrated by three examples in Fig. 1 from Gorda *et al.* [8], Al-Mamun *et al.* [24] and Fujimoto *et al.* [3]. Shown also are the central $\Delta(\varepsilon)$ values [25] in the

binary neutron stars in GW170817 [26], PSR0030+0451 [27, 28] and PSR0740+6620 [29], inferred without using any input EOS model from perturbative solutions of the dimensionless TOV equations for reduced NS variables [21]. Thus, the neutron star data do not select a unique microscopic Hamiltonian but instead reveal a universal, model-independent trace anomaly of dense matter.

What can be Bayesian inferred from nuclear collective flow data in heavy-ion collisions?— Collective flow observables [14–16] in intermediate-energy heavy-ion collisions are commonly interpreted within hydrodynamic or transport frameworks in which pressure gradients drive the acceleration of the medium [32–42]. At the level of ideal relativistic hydrodynamics, this physics [15, 43] is encapsulated in the Euler equation governing the collective velocity field \vec{v} ,

$$(\varepsilon + P) \partial_t \vec{v} = -\nabla P, \quad (3)$$

where $\varepsilon + P$ plays the role of an inertial mass density and ∇P provides the driving force. Importantly, Eq. (3) depends only on the macroscopic equation of state $P(\varepsilon)$ and is insensitive to the microscopic mechanisms that generate the pressure and energy density. We emphasize that Eq. (3) should be understood as a macroscopic organizing principle rather than a statement that the system involved in intermediate energy heavy-ion collisions behaves as an ideal fluid.

All microscopic physics—including many-body forces, short-range correlations, momentum dependence of the single-nucleon potential, in-medium scattering cross sections, or possible changes in the relevant degrees of freedom—affects the collective flow only insofar as it modifies the functional relation between P and ε . In direct analogy with the TOV equations for neutron stars, the Euler equation therefore guarantees that collective flow observables constrain the coarse-grained EOS rather than the specific microscopic Hamiltonians. In Bayesian analyses of collective flow, microscopic transport simulations are used to generate training data for emulators that span a sufficiently broad space of EOS realizations. The inference itself, however, is limited to macroscopic EOS properties that enter Eq. (3). Consequently, flow observables cannot uniquely determine the microscopic composition or interaction structure of dense matter, but instead constrain the coarse-grained EOS $P(\varepsilon)$ and its derivatives, which govern the macroscopic response of the system.

Moreover, collective flow is generated continuously throughout the entire space–time evolution of a heavy-ion collision, as demonstrated quantitatively in, e.g., Refs. [44, 45]. Pressure gradients acting at different times and spatial locations accelerate the medium locally, and the observed final-state flow represents an integral over the full dynamical history of the system. As a result, flow observables do not probe the EOS at a single energy

density, but encode a weighted average of the medium response over the range of energy densities explored during the reaction.

This averaging property can be made explicit by rewriting Eq. (3) as

$$\partial_t \vec{v} \sim -\frac{c_s^2(\varepsilon)}{1 + P/\varepsilon} \nabla \ln \varepsilon, \quad (4)$$

and integrating over the space–time evolution of the collision. The resulting collective flow therefore reflects a space–time–weighted average of the sound speed squared $c_s^2(\varepsilon)$, leading to a stronger correlation with the trace anomaly $\Delta(\varepsilon)$ than with strictly local values of $c_s^2(\varepsilon)$ at any given time. According to Eq. (2), distinct microscopic models with substantially different local $c_s^2(\varepsilon)$ profiles can thus yield the same trace anomaly $\Delta(\varepsilon)$.

Bayesian inference of the trace anomaly and speed of sound from collective flow in heavy-ion collisions.— Using a Gaussian-process emulator trained on an isospin-dependent Boltzmann–Uehling–Uhlenbeck (IBUU) transport model [46, 47] for intermediate-energy heavy-ion reactions, we recently performed Bayesian analyses [48, 49] of the excitation functions of protons’ directed and elliptic flow measured by the FOPI Collaboration at beam energies from 150 to 1200 MeV/nucleon, as well as the HADES data at 1230 MeV/nucleon [18], for mid-central Au+Au collisions. In transport simulations of heavy-ion collisions, the EOS of cold nuclear matter enters through the single-nucleon mean-field potential, while temperature-related effects are treated separately via collision integrals [34]. To account for uncertainties associated with particle scattering in dense matter, we introduced an in-medium baryon–baryon scattering cross-section (BBSCS) modification factor X (relative to free-space values) and assign it a broad prior range of $0.3 \leq X \leq 2.0$.

The mean-field potential for a baryon q is parameterized in a Skyrme-like form

$$V_q(\rho, \delta) = a \left(\frac{\rho}{\rho_0} \right) + b \left(\frac{\rho}{\rho_0} \right)^\sigma + V_{\text{sym}}^q(\rho, \delta) + V_{\text{Coul}}^q, \quad (5)$$

where $V_{\text{sym}}^q(\rho, \delta)$ denotes the symmetry potential in isospin-asymmetric nuclear matter with isospin asymmetry $\delta = (\rho_n - \rho_p)/\rho$, and V_{Coul}^q is the Coulomb potential. The parameters a , b , and σ are fixed by the saturation properties of symmetric nuclear matter (SNM) at density $\rho_0 \simeq 0.16 \text{ fm}^{-3}$. By varying the single incompressibility parameter

$$K = 9\rho_0^2 \left[\frac{d^2 E(\rho, \delta)}{d\rho^2} \right]_{\rho_0, \delta=0},$$

one systematically scans the full stiffness range of the SNM EOS at suprasaturation densities.

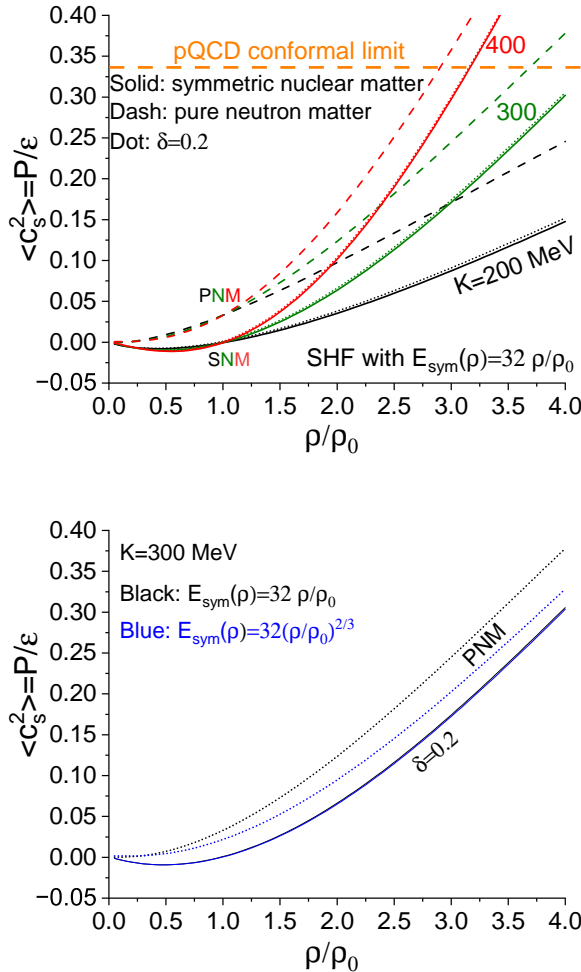


FIG. 2. The averaged speed of sound squared $\langle c_s^2(\rho) \rangle = P/\varepsilon = \phi$ as a function of reduced baryon density with a Skyrme-like EOS with varying incompressibility parameter K (upper panel) and nuclear symmetry energy (lower panel), respectively.

The corresponding energy per nucleon $E(\rho, \delta)$ in isospin-asymmetric nuclear matter is given by

$$E = \frac{3}{5} E_F^0 \left(\frac{\rho}{\rho_0} \right)^{2/3} + \frac{a}{2} \frac{\rho}{\rho_0} + \frac{b}{1+\sigma} \left(\frac{\rho}{\rho_0} \right)^\sigma + E_{sym}(\rho) \delta^2, \quad (6)$$

where E_F^0 is the nucleon Fermi energy at ρ_0 and $E_{sym}(\rho)$ is the nuclear symmetry energy. In analyzing the GSI flow data, we adopt a conservative prior range $K = 180$ – 400 MeV. As shown in the upper panel of Fig. 2, for a typical isospin asymmetry $\delta \simeq 0.2$ achievable in heavy-ion collisions and a linear $E_{sym}(\rho)$ motivated by relativistic mean-field models, the ratio $\phi = P/\varepsilon$, with $P(\rho) = \rho^2 dE(\rho, \delta)/d\rho$ and $\varepsilon = \rho E(\rho, \delta)$, spans a wide range at suprasaturation densities. Moreover, as illustrated in the lower panel of Fig. 2, varying $E_{sym}(\rho)$ within its current empirical uncertainties [50] induces only a

TABLE I. Beam energy dependence of the most probable K and X values inferred from the Bayesian analyses of FOPI’s excitation functions of protons’ directed and elliptic flow data [49].

E_{beam}/A (MeV)	K (MeV)	X
150	220 ± 55	$0.7^{+1.1}_{-0.4}$
250	320 ± 62	$0.6^{+1.3}_{-0.5}$
400	313 ± 63	$0.9^{+1.3}_{-0.8}$
600	312 ± 60	$0.9^{+1.4}_{-0.7}$
800	309 ± 63	$0.9^{+1.3}_{-0.7}$
1000	310 ± 62	$0.9^{+1.3}_{-0.7}$
1200	323 ± 53	$1.0^{+1.4}_{-0.9}$

weak effect on ϕ , reflecting the dominance of the SNM EOS in both pressure and energy density.

Finally, it is worth emphasizing that the absence of explicit momentum dependence in the single-nucleon potential allows a clean decoupling of the cold-matter EOS from thermal effects during the collision dynamics. As discussed above, the inverse Bayesian inference of the trace anomaly from collective flow is largely insensitive to microscopic composition and interaction details, and instead constrains the macroscopic EOS regardless of how it is constructed.

Listed in Table I are the most probable values of the incompressibility K and the in-medium scattering factor X inferred from our Bayesian analyses of the beam-energy dependence of protons’ directed and elliptic flow. The corresponding time evolution of the central baryon density, ρ_{cen}/ρ_0 , evaluated in a cubic cell of volume 1 fm^3 centered at the center of mass of the reaction system, is shown in Fig. 3. For each beam energy, the maximum central density attained during the collision is used to evaluate the trace anomaly, with the sound speed squared c_s^2 averaged up to this density according to Eq. (2). The systematic beam-energy dependence of the maximum central density then enables the extraction of the trace anomaly as a function of the reduced energy density, shown as green squares in Fig. 1.

Remarkably, the trace anomaly extracted from collective flow in heavy-ion collisions exhibits quantitative agreement with independent constraints inferred from neutron star observations based on mass–radius and tidal deformability measurements. This agreement arises because both systems probe the same coarse-grained EOS $P(\varepsilon)$ through integrated macroscopic responses, while remaining largely insensitive to the microscopic composition of the pressure and energy density. In the Bayesian analysis, the specific microscopic transport model used in the forward simulations serves solely as a generator of training data that spans a sufficiently broad space of EOS realizations—most notably encompassing the full range of the incompressibility parameter K —rather than as a source of model-dependent microscopic constraints. Consequently, the inferred trace anomaly reflects EOS

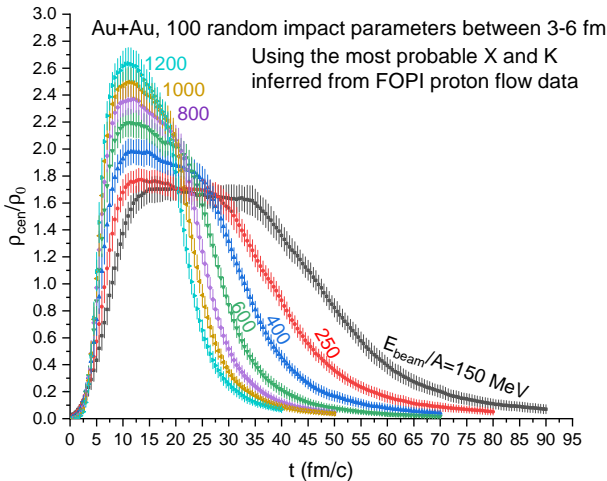


FIG. 3. Time evolution of central baryon density in mid-central Au+Au reactions with beam energies from 150 to 1200 MeV/nucleon with parameters listed in Table I.

information that is robust under changes of microscopic dynamics, explaining its consistency with independently inferred neutron star constraints.

While the matter produced in heavy-ion collisions at intermediate beam energies does not behave as a perfect ideal fluid, the transport-model framework employed here naturally incorporates non-ideal effects such as finite mean free paths and viscosity, reinforcing the robustness of the inferred trace anomaly beyond the ideal-hydrodynamic limit.

For comparison, we have also translated the $P(\rho)$ bands extracted approximately two decades ago, from kaon production data analyzed within quantum molecular dynamics (QMD) transport models [30, 31], and from collective flow data at BEVALAC and AGS energies studied using both QMD- and BUU-type transport models [32], into the trace anomaly $\Delta(\varepsilon)$ by assuming $\varepsilon = M_N \rho$, where M_N is the average nucleon mass. Interestingly, these earlier constraints from forward-modeling are generally consistent with both the neutron star $\Delta(\varepsilon)$ bands and the results extracted here from the FOPI and HADES flow data, providing additional support for the universal character of the dense-matter trace anomaly.

Having obtained the energy-density dependence of the trace anomaly $\Delta(\varepsilon)$, Eq. (2) can be inverted to recover the corresponding profile of the sound speed squared $c_s^2(\varepsilon)$ [3],

$$c_s^2(\varepsilon) \equiv \frac{dP}{d\varepsilon} = -\bar{\varepsilon} \frac{d\Delta}{d\varepsilon} + \frac{1}{3} - \Delta, \quad (7)$$

where $\bar{\varepsilon} \equiv \varepsilon/\varepsilon_0$ and $\varepsilon_0 \simeq 150$ MeV/fm³ denotes the energy density at the saturation density ρ_0 . The first term

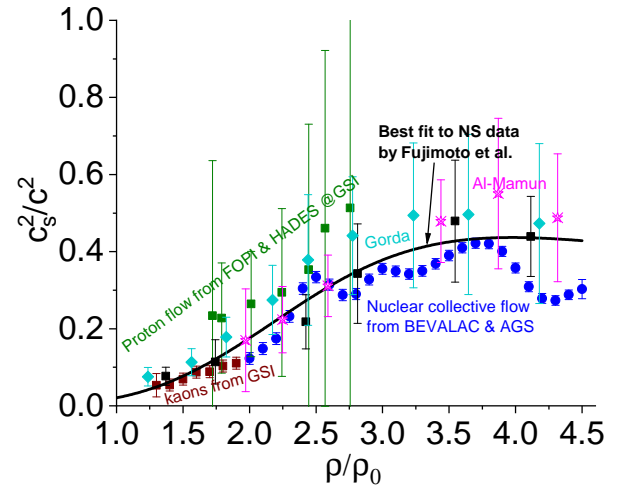


FIG. 4. Speed of sound squared derived from the trace anomaly shown in Fig. 1 using Eq. 7 in comparison with the best-fit curve inferred from neutron star observations using machine learning techniques [3].

on the right-hand side represents the derivative contribution, while the remaining terms constitute the non-derivative part. Figure 4 compares the resulting $c_s^2(\varepsilon)$ inferred from heavy-ion collisions with constraints from neutron star observations. Despite comparatively larger uncertainties arising from the derivative nature of Eq. (7) and the finite sampling of beam energies in the GSI data, the inferred $c_s^2(\varepsilon)$ values are consistent with the neutron star constraints. Overall, the mean values of $c_s^2(\varepsilon)$ from heavy-ion collisions cluster closely around the best-fit sound-speed profile obtained independently from neutron star observations using machine-learning techniques [3].

Taken together, terrestrial heavy-ion collisions and neutron star observations reveal a universal macroscopic response of dense baryonic matter, characterized by a nearly model-independent trace anomaly and a consistent sound-speed profile over the overlapping range of energy densities probed by both systems.

Conclusions.— In summary, we have performed the first Bayesian extraction of the dense-matter trace anomaly from collective flow observables in intermediate-energy heavy-ion collisions. Although these collisions generate hot, dynamically evolving matter, our transport simulations successfully decouple the cold-matter EOS through the nucleon mean-field potential from separate thermal effects handled via collision terms. This approach allows collective flow data to directly constrain macroscopic properties of the cold dense-matter EOS.

The trace anomaly inferred from these laboratory experiments shows remarkable quantitative agreement with independent constraints derived from neutron star observations, including mass-radius relations and tidal deformabilities. This consistency is particularly significant

given the vastly different data sets, priors, and inference frameworks employed.

Such nontrivial agreement demonstrates that collective flow in heavy-ion collisions and global neutron star observables probe the same coarse-grained macroscopic properties of dense matter, despite their vastly different dynamical and thermodynamic conditions. This result establishes collective flow as a laboratory-based, model-agnostic probe of dense matter that is directly complementary to neutron star observations.

Looking forward, upcoming precision measurements at next-generation heavy-ion facilities, combined with more refined neutron star data from advanced X-ray timing and gravitational-wave detectors, will further sharpen our understanding. These advancements will provide critical tests of the universality of the trace anomaly and map the dense-matter EOS across even broader ranges of energy and density.

Acknowledgement.— We thank B.J. Cai, X. Grundler, J. Margueron, W.J. Xie, and N.B. Zhang for helpful discussions. This work was supported in part by the U.S. Department of Energy, Office of Science, under Award No. DE-SC0013702.

DATA AVAILABILITY: The data that support the findings of this article will be openly available [51].

* Bao-An.Li@etamu.edu

- [1] R.C. Tolman, Proc. of the National Academy of Sciences, **20**, 169 (1934).
- [2] J.R. Oppenheimer, G.M. Volkoff, Phys. Rev., **55**, 374 (1939).
- [3] Y. Fujimoto et al., Phys. Rev. Lett. **129**, 252702 (2022).
- [4] J. Bjorken, Phys. Rev. D **27**, 140 (1983).
- [5] A. Kurkela, P. Romatschke, and A. Vuorinen, Phys. Rev. D **81**, 105021 (2010).
- [6] T. Gorda et al., Phys. Rev. Lett. **127**, 162003 (2021).
- [7] T. Gorda et al., Phys. Rev. Lett. **131**, 181902 (2023).
- [8] T. Gorda, O. Komoltsev, and A. Kurkela, Astrophys. J. **950**, 107 (2023).
- [9] O. Komoltsev and A. Kurkela, Phys. Rev. Lett. **128**, 202701 (2022).
- [10] J. Braun and B. Schallmo, Phys. Rev. D **106**, 076010 (2022).
- [11] B. Brandt, F. Cuteri and G. Endrodi, JHEP **2023**, 55 (2023).
- [12] K. Fukushima and S. Minato, Phys. Rev. D **111**, 094006 (2025).
- [13] B. J. Cai and B. A. Li, Eur. Phys. J. A **61**, no.3, 55 (2025).
- [14] P. Danielewicz and G. Odyniec, Phys. Lett. **B157**, 146 (1985).
- [15] J. Y. Ollitrault, Phys. Rev. D **46**, 229 (1992).
- [16] A. Poskanzer and S.A. Voloshin, Phys. Rev. C **55**, 1671 (1998).
- [17] W. Reisdorf et al. [FOPI], Nucl. Phys. A **876**, 1 (2012).
- [18] J. Adamczewski-Musch et al. [HADES], Eur. Phys. J. A **59**, 80 (2023).
- [19] J. Saes, R. Mendes, and N. Yunes, Phys. Rev. D **110**, 024011 (2024).
- [20] M. Marczenko, Phys. Rev. C **110**, 04581 (2024).
- [21] B.J. Cai, B.A. Li, and Z. Zhang, Astrophys. J. **952**, 147 (2023).
- [22] B.J. Cai, B.A. Li, and Z. Zhang, Phys. Rev. D **108**, 103041 (2023).
- [23] B. J. Cai, B. A. Li and Y. G. Ma, [arXiv:2601.02980].
- [24] M. Al-Mamun et al., Phys. Rev. Lett. **126**, 061101 (2021).
- [25] B.J. Cai and B.A. Li, Phys. Rev. D **112**, 023023 (2025).
- [26] B. Abbott et al., Phys. Rev. Lett. **121**, 161101 (2018).
- [27] T. Riley et al., Astrophys. J. Lett. **887**, L21 (2019).
- [28] M. Miller et al., Astrophys. J. Lett. **887**, L24 (2019).
- [29] T. Salmi et al., Astrophys. J. **941**, 150 (2022).
- [30] C. Fuchs, Prog. Part. Nucl. Phys. **56**, 1-103 (2006).
- [31] W. G. Lynch, et al., Prog. Part. Nucl. Phys. **62**, 427 (2009).
- [32] P. Danielewicz, R. Lacey, W. G. Lynch, Science 298, 1592 (2002).
- [33] H. Stöcker and W. Greiner, Phys. Rep. **137**, 277 (1986).
- [34] G.F. Bertsch and S. Das Gupta, Phys. Rep. **160**, 189 (1988).
- [35] W. Cassing, V. Metag, U. Mosel and K. Niita, Phys. Rep. **188**, 363 (1990).
- [36] W. Reisdorf and H.G. Ritter, Ann. Rev. Nucl. Part. Sci. **47**, 663 (1997).
- [37] S.A. Bass et al, Prog. Part. Nucl. Phys. **41**, 255 (1998).
- [38] O. Buss, et al., Phys. Rept. **512**, 1 (2012).
- [39] U. Heinz and R. Snellings, Ann. Rev. Nucl. Part. Sci. **63**, 123 (2013).
- [40] W. Trautmann and H. H. Wolter, Int. J. Mod. Phys. E **21**, 1230003 (2012).
- [41] A. Sorensen, et al., Prog. Part. Nucl. Phys. **134**, 104080 (2024).
- [42] Y. J. Wang and Q. F. Li, Front. Phys. (Beijing) **15**, no.4, 44302 (2020).
- [43] P. Danielewicz, Nucl. Phys. A **685**, 368 (2001).
- [44] P. Li, Y. Wang, Q. Li and H. Zhang, Phys. Lett. B **828**, 137019 (2022).
- [45] T. Reichert and J. Aichelin, Phys. Rev. C **111**, no.5, 054916 (2025).
- [46] B. A. Li, C. B. Das, S. Das Gupta and C. Gale, Phys. Rev. C **69**, 011603 (2004); *ibid*, Nucl. Phys. A **735**, 563 (2004).
- [47] B. A. Li, L. W. Chen and C. M. Ko, Phys. Rep. **464**, 113 (2008).
- [48] B. A. Li and W. J. Xie, Nucl. Phys. A **1039**, 122726 (2023).
- [49] B. A. Li and W. J. Xie, Phys. Rev. C **111**, no.5, 054602 (2025).
- [50] B. A. Li, arXiv:2510.05508, Euro Phys. J. Special Topic on High-Density Nuclear Matter, in press (2026).
- [51] Bao-An Li, 2025, "Bayesian Analyses of FOPI Proton Flow Data", <https://doi.org/10.7910/DVN/DUVT52>, Harvard Dataverse, V1